

INFLUENCE OF THROTTLING AND SYNTHETIC JETS ON SPECTRAL PROPERTIES AND PRESSURE PULSATIONS LEVEL IN THE AIR INTAKE INTEGRATED WITH THE AIRFRAME USING RANS/ILES METHOD

L. Benderskiy¹, D. Lyubimov¹, A. Terekhova¹.

DALyubimov@yandex.ru, alexa.terekhova@yandex.ru

¹Central Institute of Aviation Motors, Moscow

Motivation:

A thick boundary layer enters the inlet of the air intake (AI) in the power plants integrated with the airframe. It was formed on the elements of the aircraft. It is important to know for practice, the effect of the location of the AI and its geometry on the flow and turbulence characteristics at the entrance to the engine compressor. Experimental investigation of flows is a technically complex and costly task in such AI. The use of vortex-resolving methods in contrast to the RANS methods makes it possible to obtain not only the averaged flow parameters but also the spectral properties of the pressure pulsations in the AI, which change when the operating mode changes.

Goal of the work:

Analysis of spectral properties and pressure pulsations level in a subsonic AI integrated with an airframe of an aircraft with different throttling rate and using synthetic jets (SJ).

The calculations were carried out by RANS/ILES high-resolution method

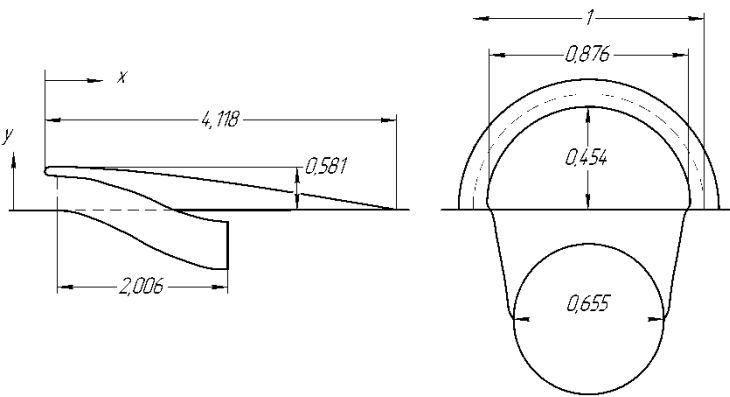
Main features (Lyubimov D.A. High Temperature, Vol. 50, No. 3, pp. 420-436., 2012):

- Roe's flux difference splitting method.
- **Monotonicity-preserving scheme MP9** [A. Suresh, H.T. Huynh, JCP 1997, V.136, P.83-99] with upwind 9th-order approximation in smooth regions for calculating flow parameters on cell faces. It makes possible to calculate supersonic flows with shocks without modification of the method.
- LES with implicit SGS-model (ILES): the scheme viscosity performs a function of a subgrid scale (SGS) model.
- the transition from RANS to ILES is achieved by putting to 0 the turbulent viscosity ν_t , and this is achieved by modifying the distance in the Spalart-Allmaras turbulence model:
- the modified distance d_{ILES} was calculated using formulas:

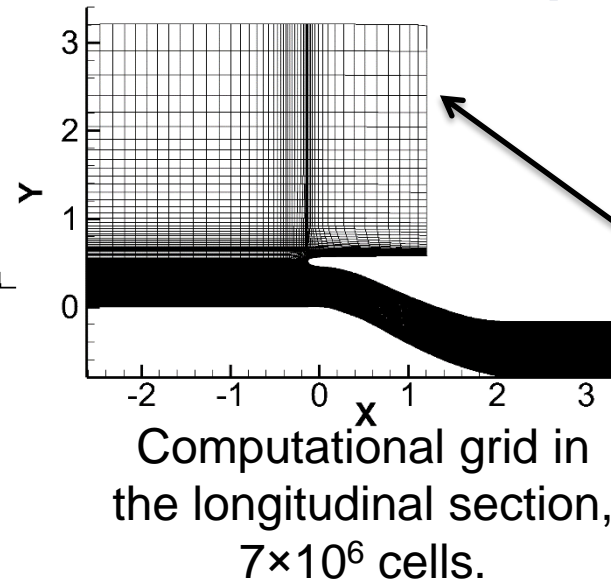
$$\begin{aligned}d_{ILES} &= d, \text{ for } d \leq C_{ILES} \Delta_{\max}, \\d_{ILES} &= 10^{-6}H, \text{ for } d > C_{ILES} \Delta_{\max},\end{aligned}$$

where H is the characteristic size of the task, Δ_{\max} is the maximum size of the current cell, $C_{ILES}=0.65$ – only determines the position of the transition from RANS to ILES

Formulation of the problem



Geometry of the AI



Mode parameters (report [1]):

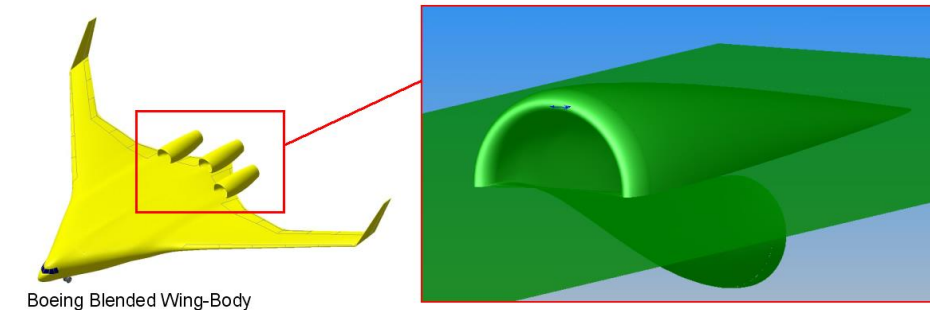
$$M=0.83, Re=1.3 \cdot 10^6$$

$$P_{in}^* = 220632 \text{ Pa}$$

$$T_{in}^* = 144.4 \text{ K}$$

$$P_{outlet} = 140431 \text{ Pa}$$

$$P_{out} = \text{var}$$

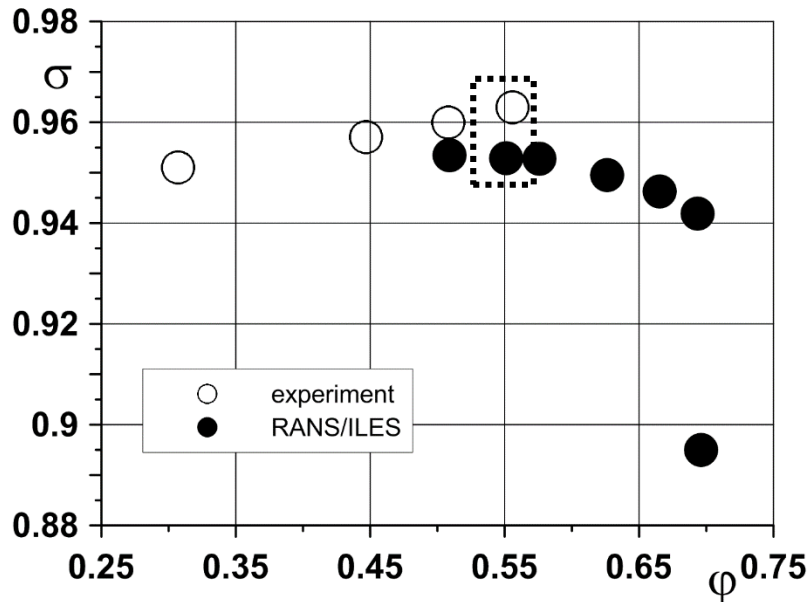


Location scheme of the AI

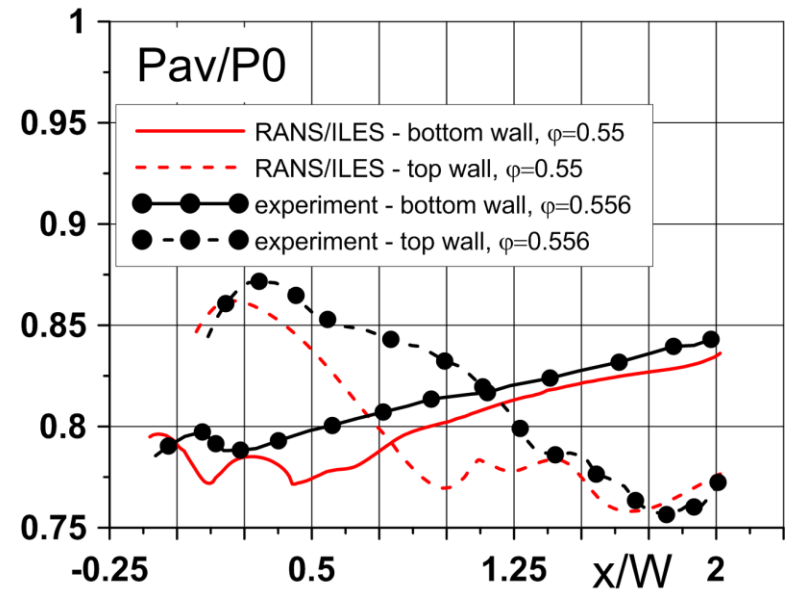
The static pressure at the outlet from the channel was varied to obtain the throttling of the AI.

All linear dimensions were referenced to the W . W is the width of the entrance to the AI.

- ❑ A flat plate was used as a simulator of the airframe. On the plate was mounted AI. At the entrance to the calculation area, a boundary layer with a thickness $\delta/W=0.1544$ was set, whose profile was close to the one of the turbulent boundary layer.



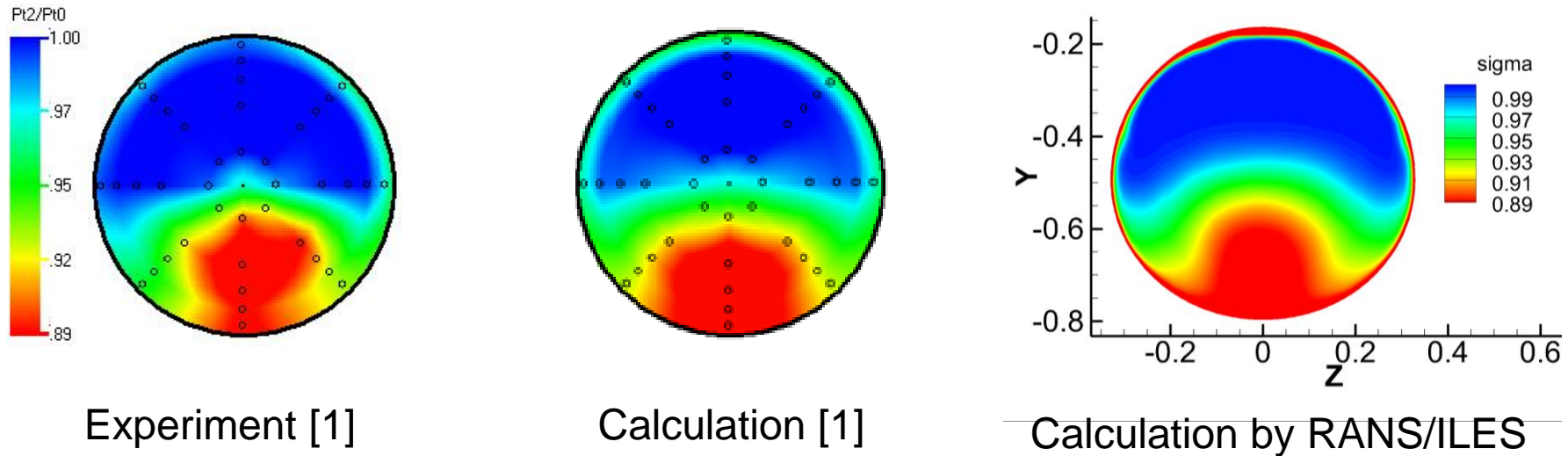
Performance curve for the AI outlet.
Comparison of the calculation and experiment.



The distribution of static pressure along the top and bottom walls of the AI. Comparison of the calculation and experiment.

- In the vicinity of the outlet section, a satisfactory match is observed between calculation and experiment

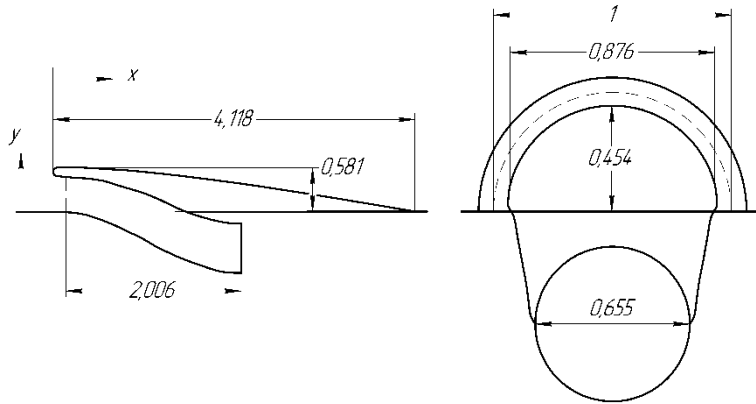
Comparison with experiment and calculation [1] of the pressure recovery coefficient in the outlet section of the AI



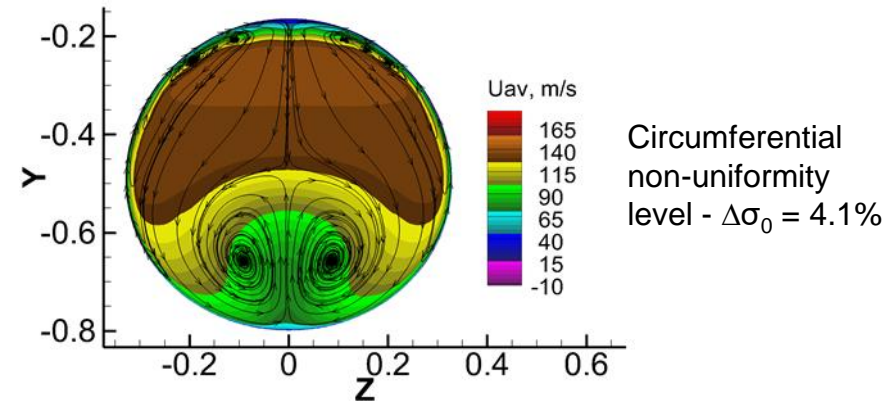
Total pressure loss coefficient fields in the outlet section of the AI

- The calculation by the present method is in satisfactory match with the experimental and calculation data from [1] (in this work the calculation was carried out using the RANS method).

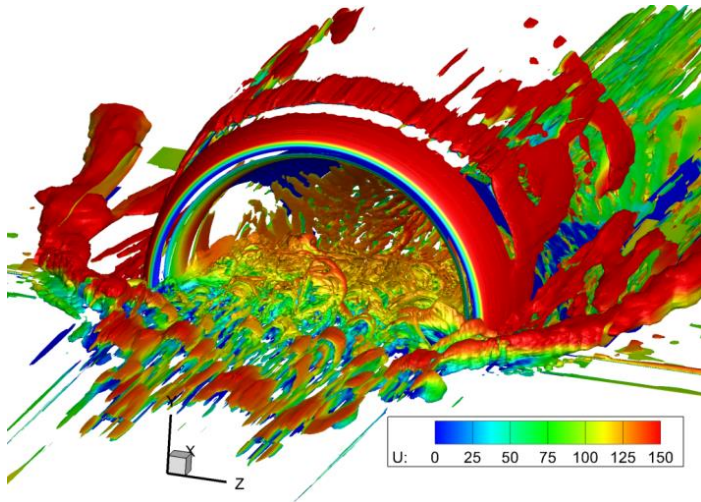
Peculiar properties of the flow in the AI and the reasons for their occurrence



Geometry of the AI

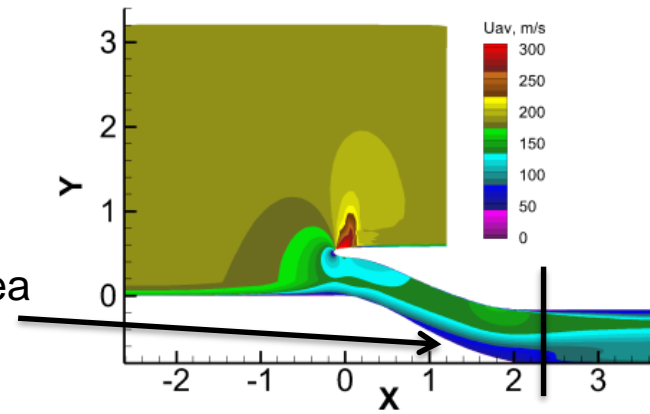


There is a cardinal change of the flow in the AI. It is caused because of two factors. It is D-shaped in the inlet and round in the outlet. In the longitudinal section, the AI diffuser is S-shaped. These factors lead to the formation of two longitudinal vortices of high intensity in the AI, which transfer a low-velocity and low-energy flow from the walls of the diffuser to the core of the flow.



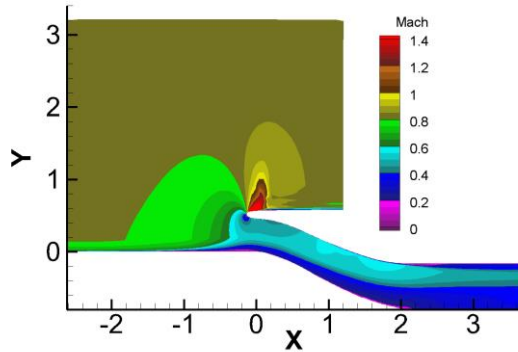
A thick turbulent boundary layer enters the AI entrance.

(The constant value surface of the Q-criterion)

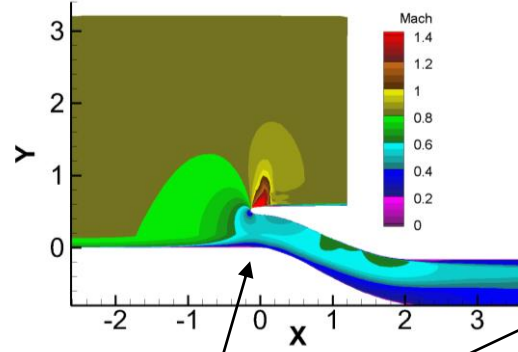


Low-speed area

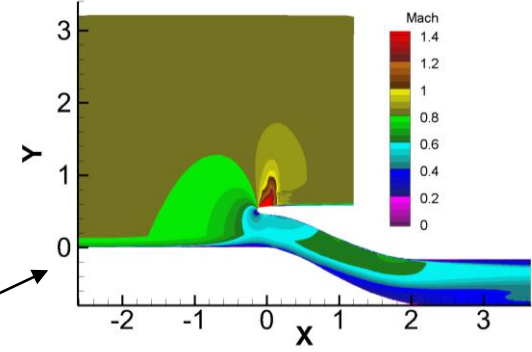
$\varphi=0.509$



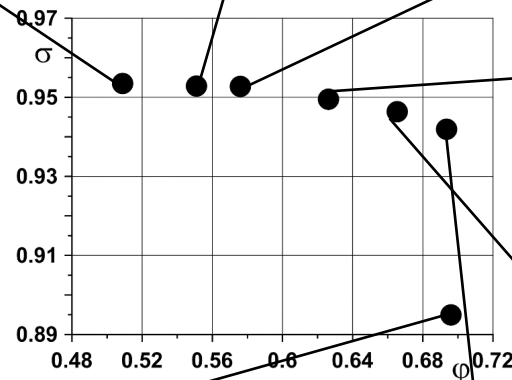
$\varphi=0.554$



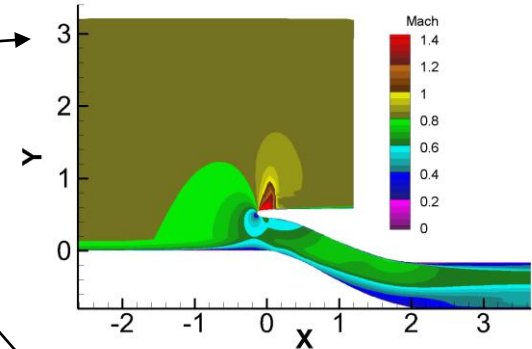
$\varphi=0.576$



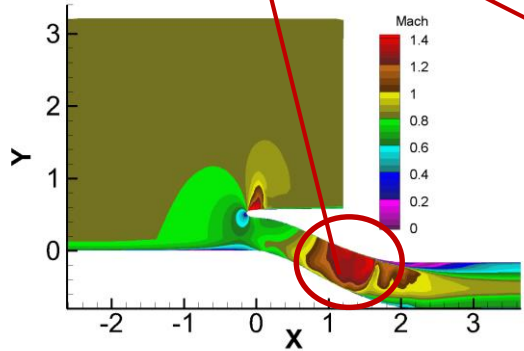
Supersonic areas
causing peaks of
pressure pulsations near
the top and bottom walls



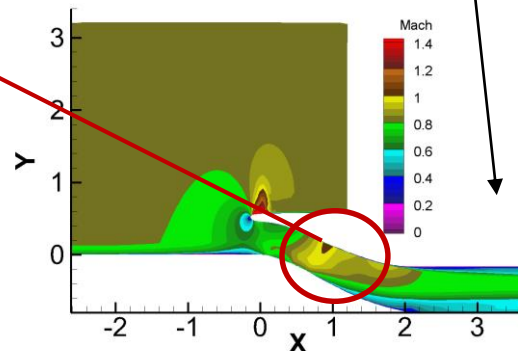
$\varphi=0.626$



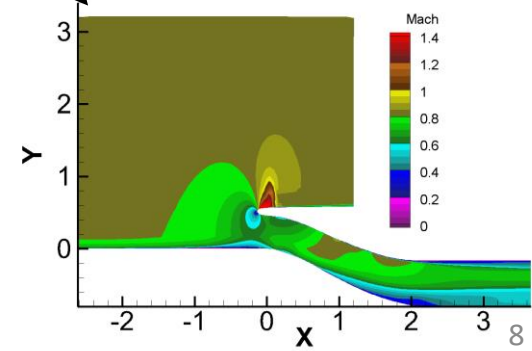
$\varphi=0.696$



$\varphi=0.693$

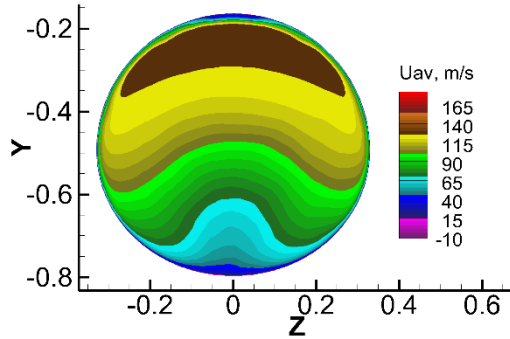


$\varphi=0.665$

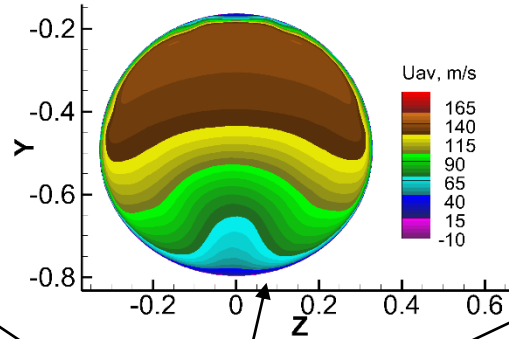


Throttling influence on the fields of the averaged velocity and the cross section averaged circumferential non-uniformity at the $x/W=2.064$

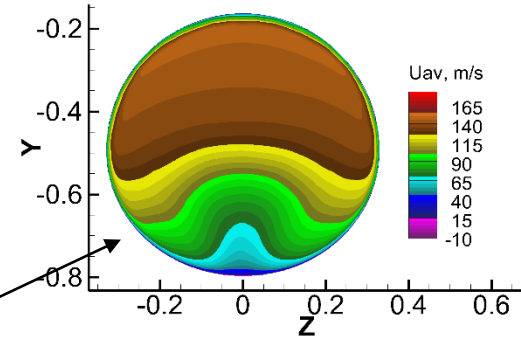
$\varphi=0.509$, $\Delta\sigma_0 = 3.5$ %



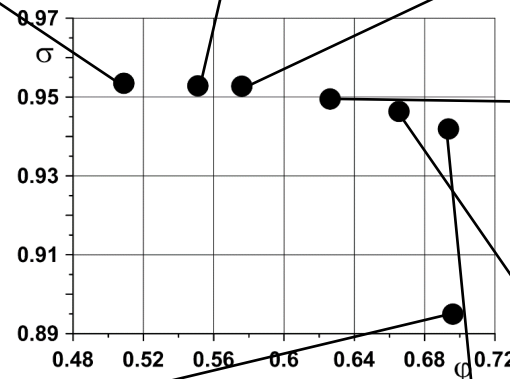
$\varphi=0.554$, $\Delta\sigma_0 = 4.2$ %



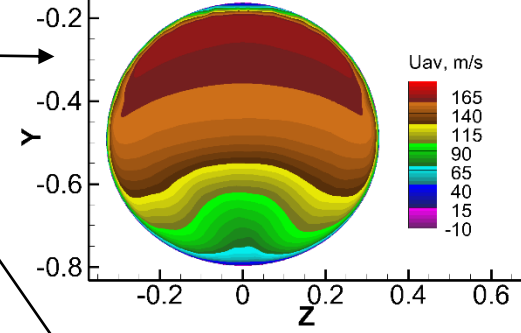
$\varphi=0.576$, $\Delta\sigma_0 = 4.1$ %



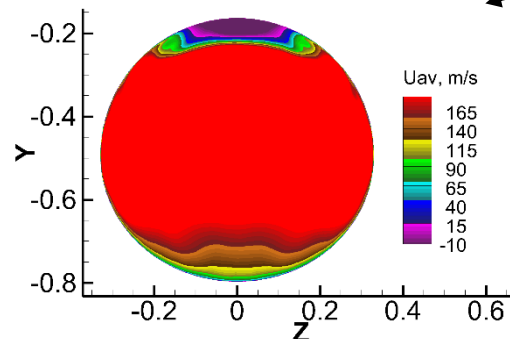
The non-uniformity level of total pressure loss coefficient increases as the throttling rate increases!



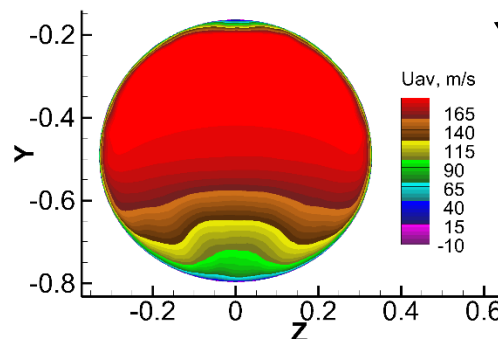
$\varphi=0.626$, $\Delta\sigma_0 = 5.3$ %



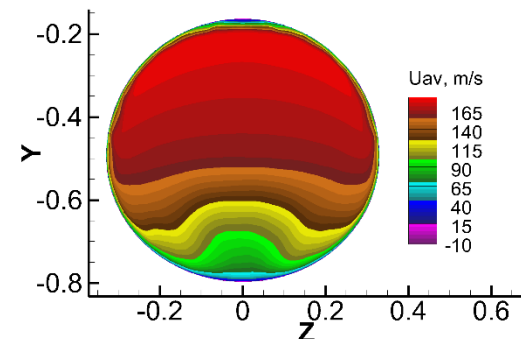
$\varphi=0.696$, $\Delta\sigma_0 = 12.5$ %



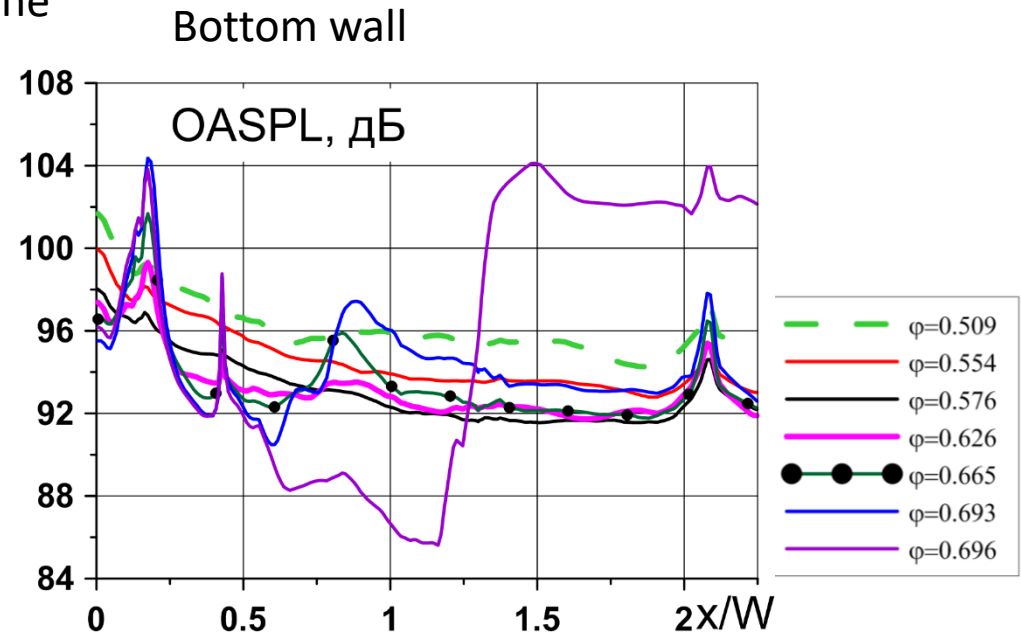
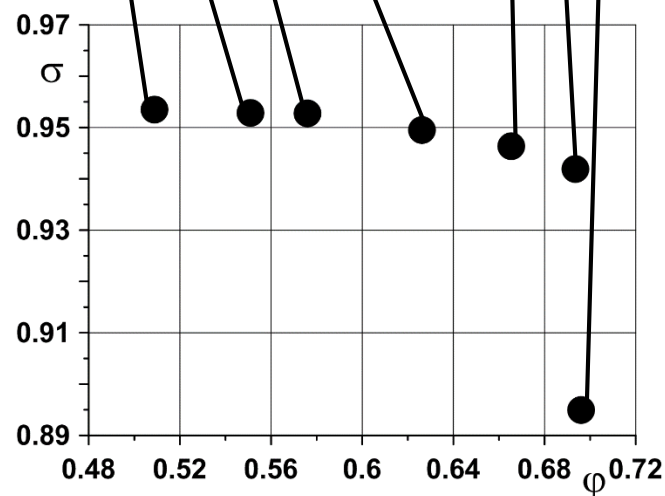
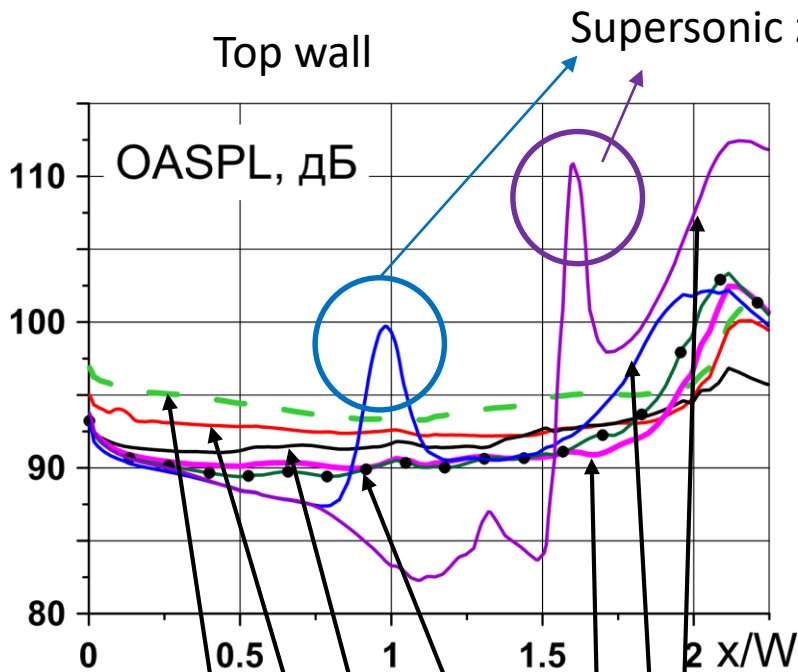
$\varphi=0.693$, $\Delta\sigma_0 = 6.3$ %



$\varphi=0.665$, $\Delta\sigma_0 = 5.8$ %

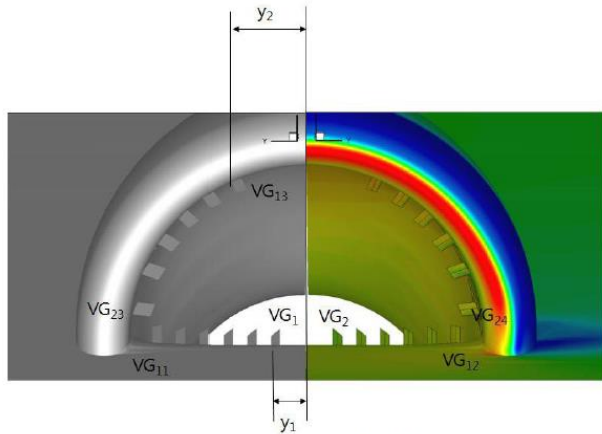


Throttling influence on the integral level of pressure pulsations along the top and bottom walls of the AI



For the values $\phi \leq 0.665$, the distribution of pressure pulsations along the top wall is qualitatively similar. For $\phi > 0.665$, pulsation peaks appear. The reason of it is the emergence of the supersonic areas, peaks appear in the places of these supersonic regions. On the bottom wall, the peaks begin to appear at $\phi \geq 0.626$.

The derivative of the longitudinal generatrix of the channel AI is destroyed in the output section. The curvilinear shape of the diffuser in the transverse direction turns into a circular one, and there is a slight increase of pressure pulsations level, which is characteristically of all the investigated ϕ .



(a) Front view of installed VGs

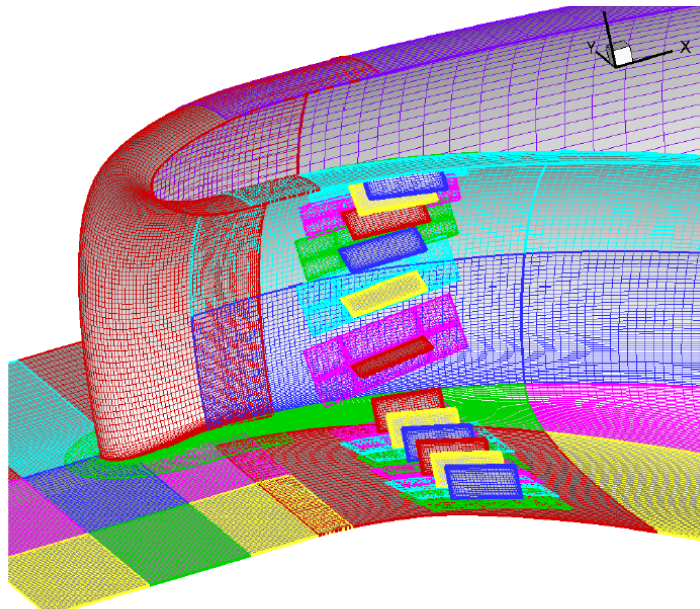


Figure 1. Overset mesh system for BLI-inlet and VGs.

AIAA-2010-842

Plate vortex generators

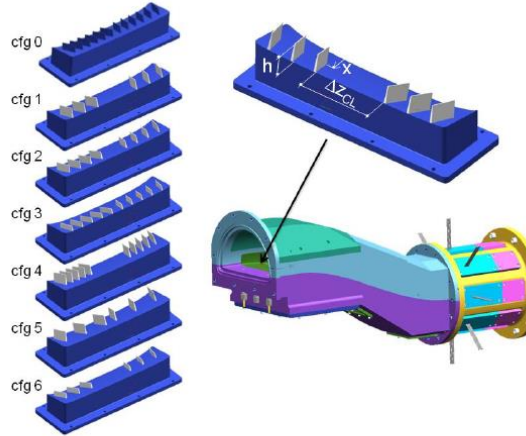


Figure 10. Schematics of the seven DOE configurations for the passive flow control.

AIAA-2011-35



Inlet A with fences installed

AIAA 2004-0764

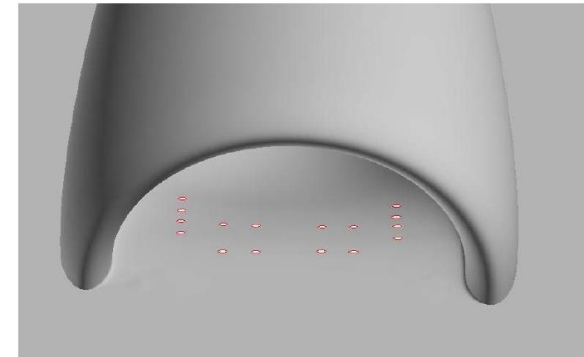
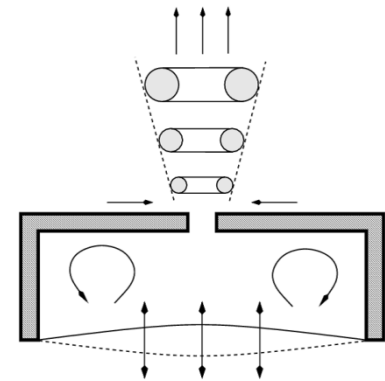


Figure 3. View of the 16 jets making up Configuration 10

AIAA-2010-841

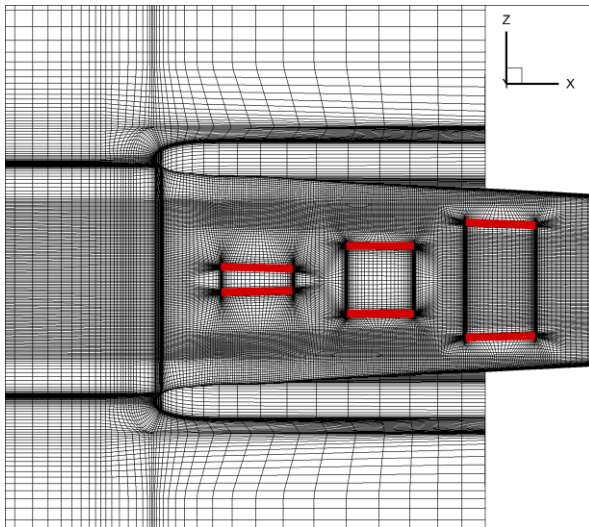
Scheme of the synthetic jets (SJs) generator



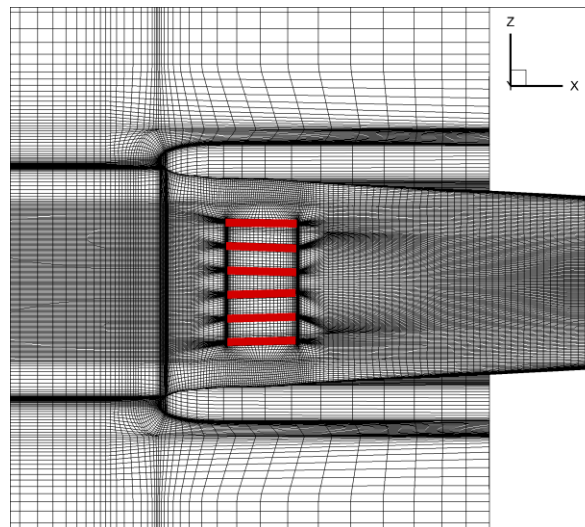
To save computing resources, the SJs generator was modeled by boundary conditions on the wall: $Q_n = a \times \sin(\omega t)$.

Variants of the slots location for the SJ exit

- There were considered about 20 variants of the SJs. One of the most effective were variants with the SJs location **reverse_pyramid (N1)** and **middle_angle (N2)** with amplitude $q=150$ m/s, frequency $f=100$ Hz, so their results will be presented further. The parameters of the SJs were selected on the basis of [2].



№1 - reverse_pyramid



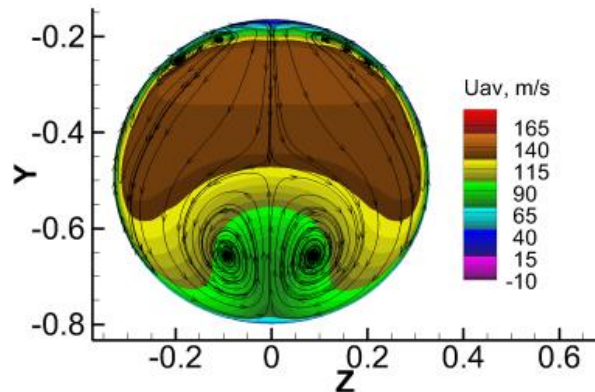
№2 - middle_angle

- SJs with a relatively low frequency were used: 100-250 Hz. Such low-frequency jets affect on the flow likewise plate vortex generators: each jet creates a pair of opposite-directional vortices.
- A high-frequency SJs acts on the flow as a usual continual jet. Analysis showed, that their use did not lead to a positive result and they do not presented here.

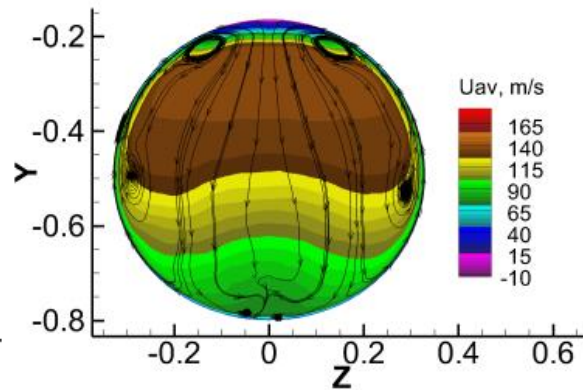
SJs location	$c_{\mu}, \%$
middle_angle	0.443
reverse_pyramid	0.657

Influence of the synthetic jets position on the averaged longitudinal velocity and total pressure losses coefficient in the outlet section

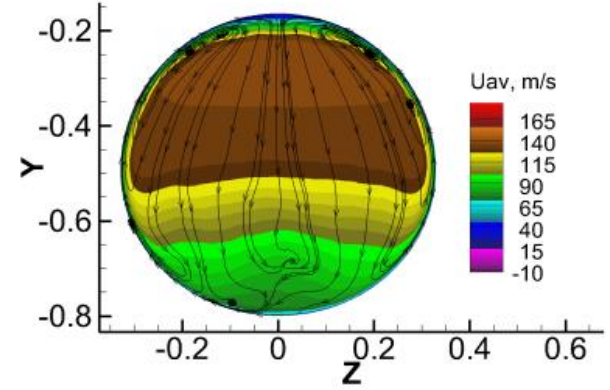
without SJs



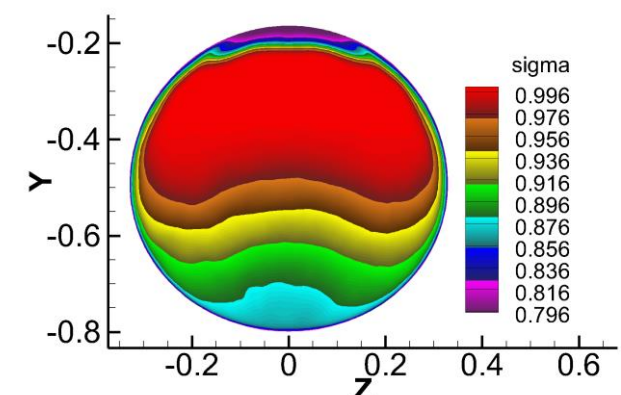
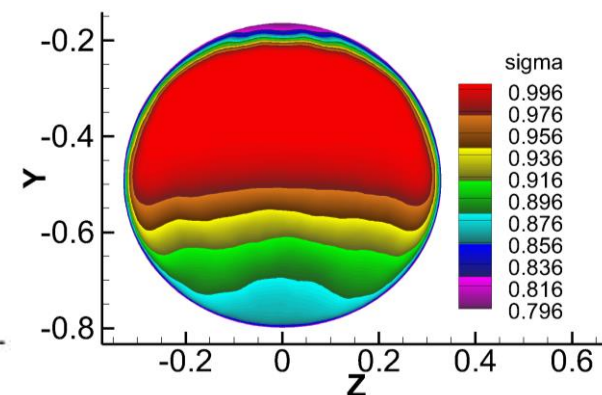
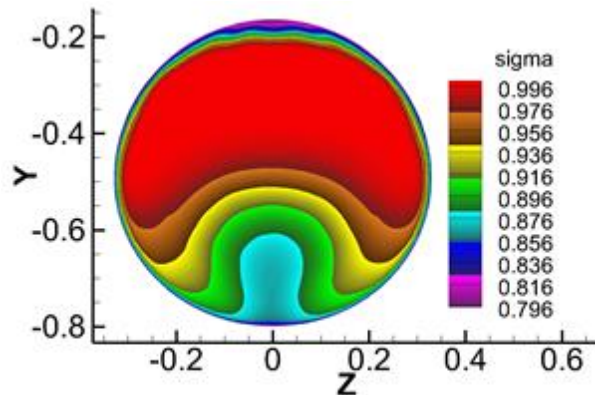
№1 reverse_pyramid



№2 middle_angle



- SJs destroy pair of the vortices in the lower part of the section, as a result of which the non-uniformity distribution of parameters decreases in the circumferential direction

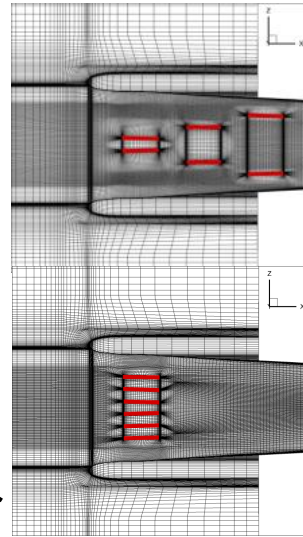
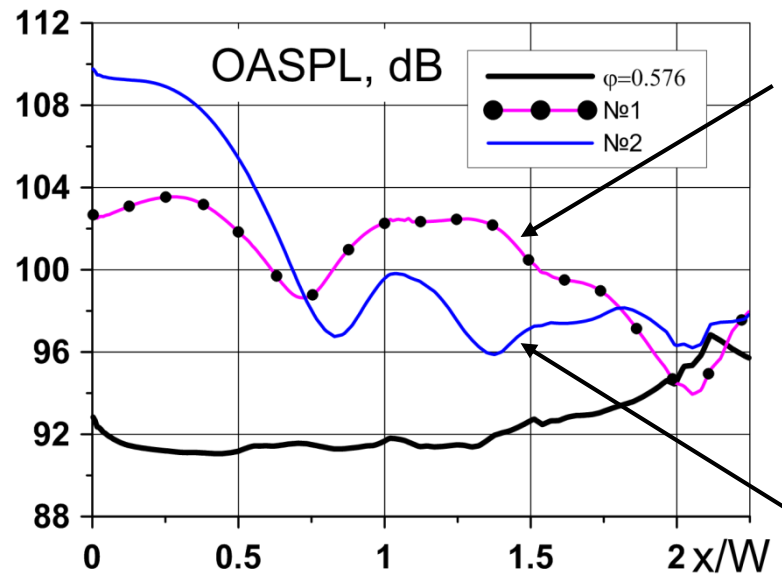


- There is a decrease in circumferential non-uniformity of total pressure loss coefficient

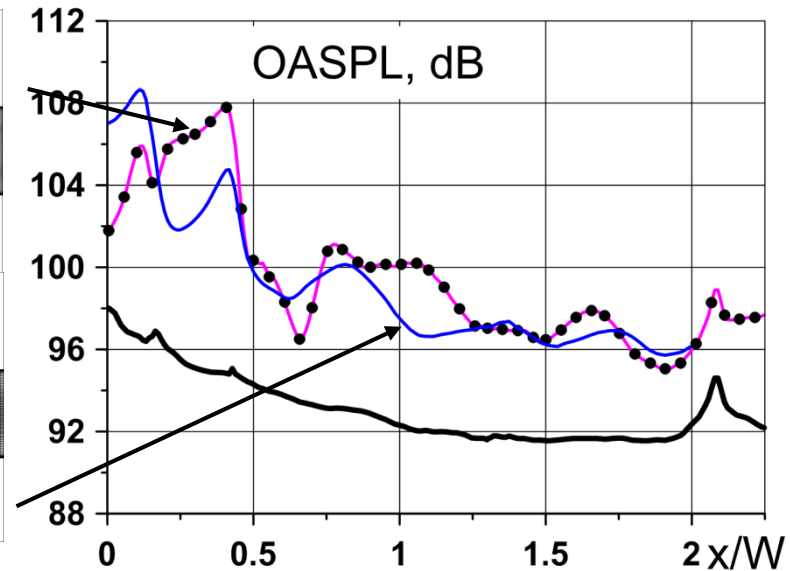
Influence of the SJs parameters on the integral level of pressure pulsations along the top and bottom walls

№1

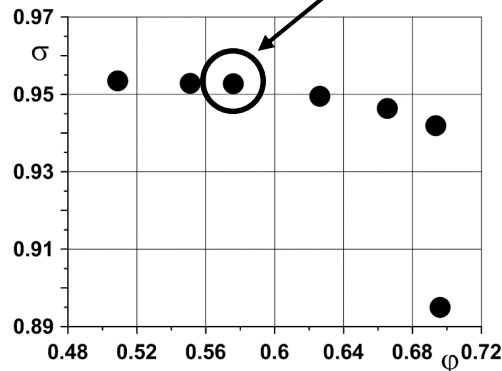
bottom walls



№2

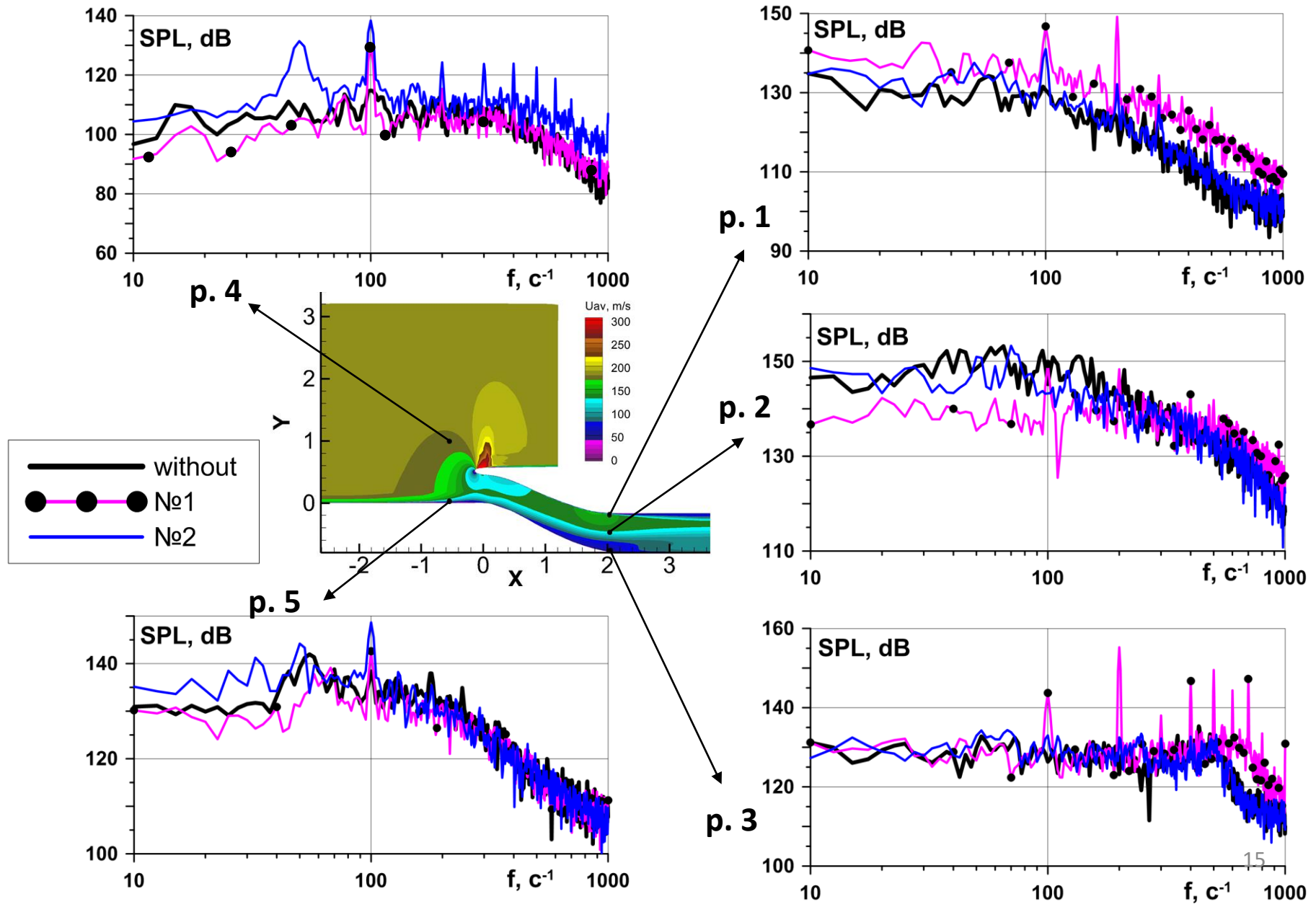


Operating mode - $\varphi=0.576$



It can be seen that the pressure pulsations level increases with using of synthetic jets and the curves qualitatively have a different character for different regimes. Nevertheless, on the top wall in section $x/W=2$ the pulsations level does not change, but on the bottom wall it increases by 4 dB. The peak area is saved for both variants.

Influence of the SJs parameters on spectral properties at characteristic points



- Analysis of the results of the RANS/ILES high-resolution method showed that it provides a satisfactory coincidence in the distribution of the pressure recovery coefficient in the AI outlet section with the experimental data and the RANS calculations of other authors.
- It was considered about 20 variants of SJs. There were found regime parameters and the positions of the slots for their blowing, which ensured the reduction of the circumferential non-uniformity of total pressure loss coefficient in the AI outlet section. In this case, SJs destroy pair of vortices in the lower part of the AI outlet section.
- The best results were given by variants with an amplitude $q = 150$ m/s and a frequency $f = 100$ Hz.
- With a decrease in the throttling rate supersonic regions appear, that cause peaks in the integral level of pressure pulsations.
- Pressure pulsations level increases with using of SJs and the curves qualitatively have a different character. Nevertheless, on the top wall in section $x/W=2$ the pulsations level does not change, but on the bottom wall it increases by 4 dB. The peak area is saved for both variants.
- SJs cause pulsations peaks in the outlet section on the upper wall, at a frequency of 100 Hz and several of its harmonics. At the same time, the pulsations level climbs in option № 1 much higher than in option №2.
- On the bottom wall, SJs №2 practically does not increase the pulsations level in comparison with the no-jets option, while SJ №1 increases them significantly.
- In the core of the flow, SJ №1 reduce low-frequency pulsations on the AI outlet.
- At the AI entrance (points 4, 5), it can be seen that SJs affect the flow upstream, causing pulsations with a certain oscillation frequency, the low-frequency oscillations of SJ № 2 are higher than №1 and higher than the no-jets variant. SJ №1 at frequencies below the jet frequency reduce pulsations. Both SJs variants increase the pulsations level for these points in comparison with the no-jets option at frequencies above the jet frequency. It is worth noting the pulsations peaks of SJ №2 at a frequency lower than the natural frequency of the SJs.

1. Berrier B.L., Carter M.B., and Allan B.G. High Reynolds Number Investigation of a Flush-Mounted, S-Duct Inlet with Large Amounts of Boundary Layer Ingestion // NASA/TP. 2005. №213766. 170P.
2. D. A. Lyubimov and I. V. Potekhina, «Application of the RANS/ILES Method in Analyzing the Efficiency of the Control of Separation Flows in Diffusers Using Synthetic Jets,» ISSN 0015-4628, Fluid Dynamics, 2015, Vol. 50, No. 4
3. Lyubimov, D.A. Development and application of a high-resolution technique for Jet flow computation using large eddy simulation, High Temperature, 50(3), (2012).

Thanks for attention